MICROFABRICATED TUNABLE BENDING STIFFNESS DEVICE

Osamu Tabata, Satoshi Konishi, Pierre Cusin, Yuuichi Ito, Fumie Kawai,
Shinichi Hirai and Sadao Kawamura
Ritsumeikan University
Noji-higashi, Kusatsu-shi, Shiga-ken, 525-8577 JAPAN
E-mail: tabata@se.ritsumei.ac.jp, TEL: 81-77-561-2882, FAX: 81-77-561-2665

ABSTRACT

This paper reports a device with tunable bending stiffness realized by microfabrication technology. Based on the newly proposed principles, two types of devices whose bending stiffness were controlled by electrostatic force and pneumatic force were fabricated. From the analysis and experiments, the feasibility of the proposed principles were confirmed and the performances of the prototyped devices were demonstrated.

INTRODUCTION

In areas such as welfare, rehabilitation and sports training, deformable actuators characterized by a high power to weight ratio, namely soft actuators, are strongly required to support human motion [1-3]. Such soft actuators offer a natural compliance, making them human being compatible, while showing the possibility for several DOE (Degree of Freedom) to be controlled.

To realize these soft actuators, the device with tunable bending stiffness is expected to play an important role as schematically shown in Fig.1. The devices are attached on a deformable shell and act as the soft actuator. This soft actuator supports a joint of a human and used to constrain the human motion.

In this paper, we propose two types of device with tunable bending stiffness controlled by electrostatic force or pneumatic force. The concept of deformable pneumatic actuator will be explained first. Then, analysis of the device characteristic using electrostatic force, structures of the devices, fabrication process and measured performances of the prototyped devices will be reported.

CONCEPT OF A DEFORMABLE PNEUMATIC ACTUATOR

The deformable shell concept using micro devices is shown in Fig.2. The motion of a deformable shell is determined by the configuration of mechanical

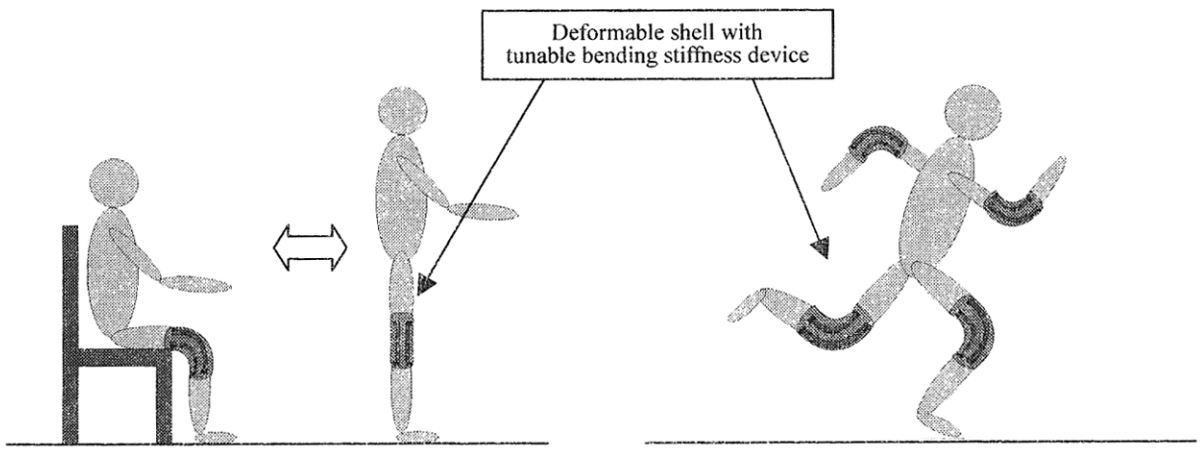

Fig.1 Apparatus to support human motion in welfare, rehabilitation and sports training using tunable bending stiffness devices.

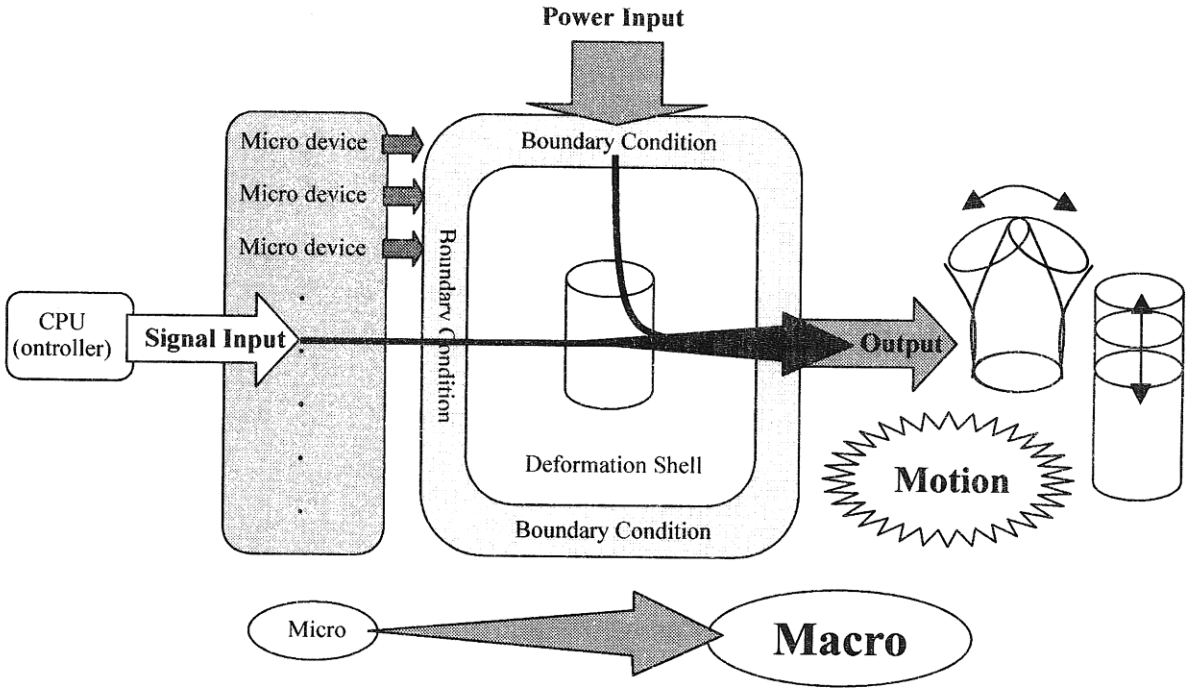

Fig.2 Concept of the deformable shell using micro devices.

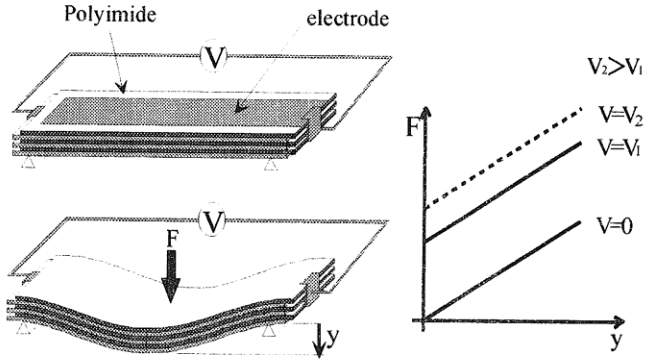

Fig.3 structure and characteristics of a electrostatically controlled device.

constraints on its shell. These constraints are act as the boundary condition of the deformable shell. For example, if the bending stiffness of one side of the deformable shell wall is constrained, the deformable shell bends toward this direction by pressurizing the deformable shell. If the stretching of the deformable shell wall is constrained, the deformable shell is difficult to expand by pressurizing the deformable shell. Various combinations of constraint sets could be possible regarding the bending and stretching.

The proposed devices in this report will be used to define the bending stiffness as a mechanical constraint according to external control signals.

By miniaturizing the device size and arranging them in stacked or arrayed form, the performance of the apparatus can be improved as shown in this paper. This concept utilizing passive element is different from the conventional approach using the actuators with electrostatic force or pneumatic force [4, 5]. This approach provides new possibility to control the motion in macro world by using micro devices.

ELECTROSTATIC STACKED FILM DEVICE

DESIGN

Figure 3 schematically shows the structure and characteristics of an electrostatically controlled device. The device is composed of stacked flexible polyimide thin films with patterned Ni electrodes. The electrodes are connected to positive and negative high voltage source alternately. Since the electrostatic force between each film generates friction force, the required force to bend the stacked film structure increases with increasing the applied voltage.

The relationship between force (F) and displacement (y) was derived theoretically as Eq.(1).

$$F = \frac{16Ew_f h^3}{n^2 L^3} y + \frac{\varepsilon_r \varepsilon_0 n^2 V^2 w_e \mu}{h} \qquad (1)$$

where w_f is film width, L is film length, E is film Young`s modulus, h is total thickness of the stacked structure, n is a number of the film (film thickness =

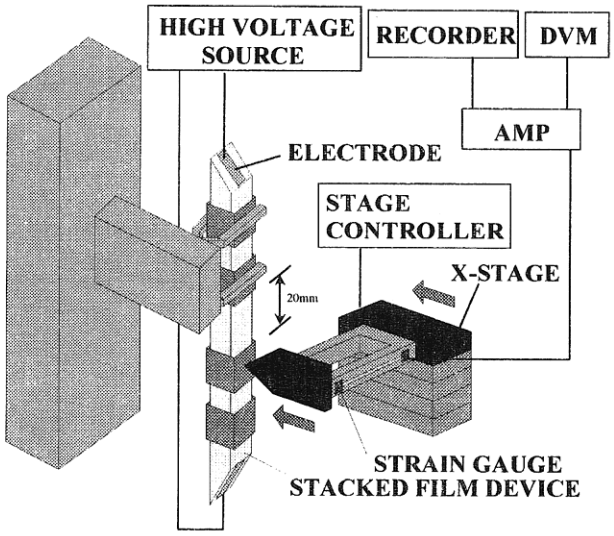

Fig.4 Measurement setup of a electrostatically controlled device.

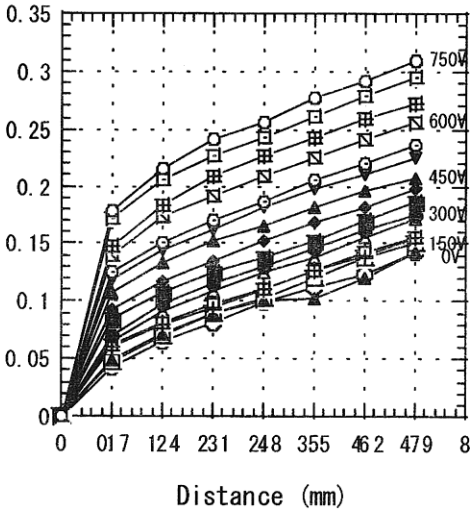

Fig.5 Measured results for the device with n of 200, w_f of 10 mm, w_e of 6 mm, L of 20 mm and h of 5.4 mm.

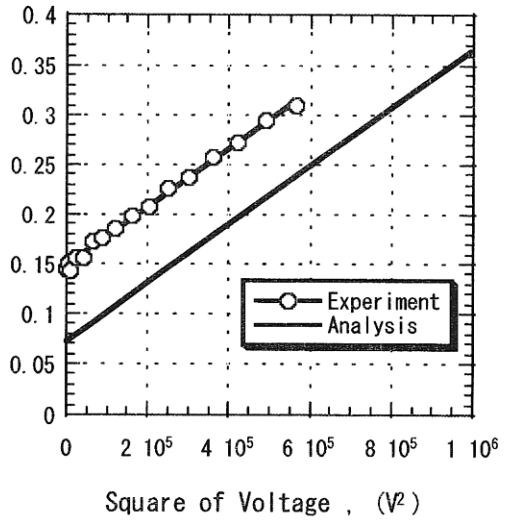

Fig.6 Measured relationship between force and V^2.

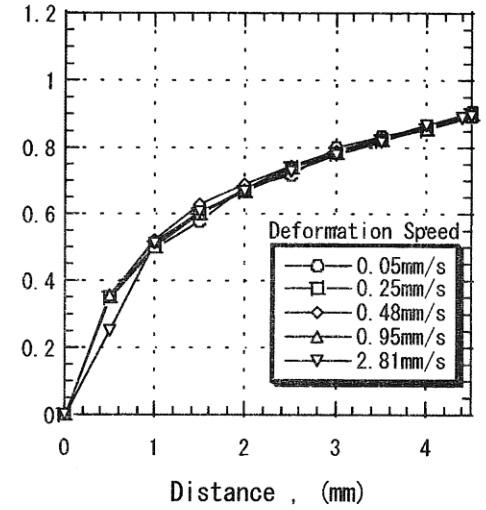

Fig.7 Measured relationship between force and distance with varying the deformation speed with applied voltage of 750V.

h/n), V is applied voltage, ε_r is specific dielectric constant of the film, ε_0 is dielectric constant of vacuum, w_e is width of the electrode and μ is dynamic friction coefficient.

Since the second term of the equation that relates to a friction force between the films is proportional to n^2, making the film thinner improves the tunable range of the bending stiffness.

EXPERIMENTS

Figure 4 shows the measured results for the device with n of 200, w_f of 10 mm, w_e of 6 mm, L of 20 mm and h of 5.4 mm. The required force to bend the stacked film structure was measured by pushing the one end of the device by a probe with a strain gauge. The required force to bend the stacked film structure increases with increasing the applied voltage as shown in Fig.5.

Figure 6 shows the measured relationship between force and V^2. The measured force was proportional to the V^2 as predicted by theoretical calculation shown in Eq. (1). The discrepancy between the measured results and the theoretical calculation is caused by the fact that the friction between each film at applied voltage of zero is neglected in the theoretical calculation.

The relationships between force and distance were

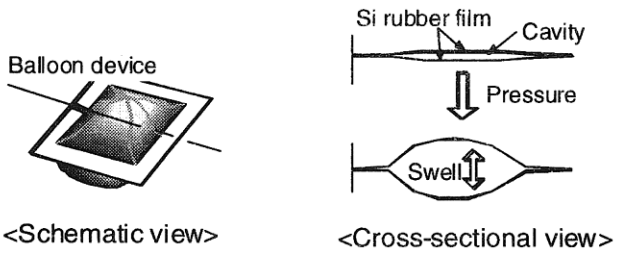

Mechanism of the balloon device

Fig.8 Principle of pneumatically controlled device.

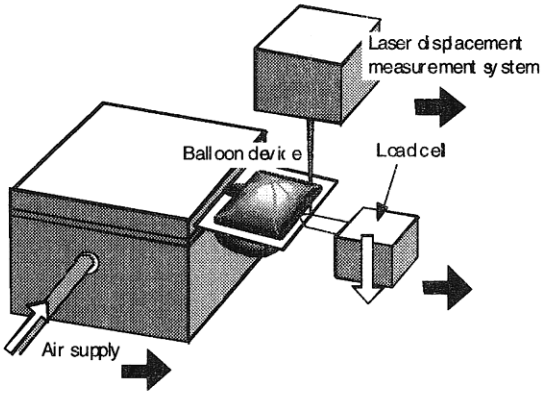

Fig.9 Experimental setup of the pneumatically controlled device.

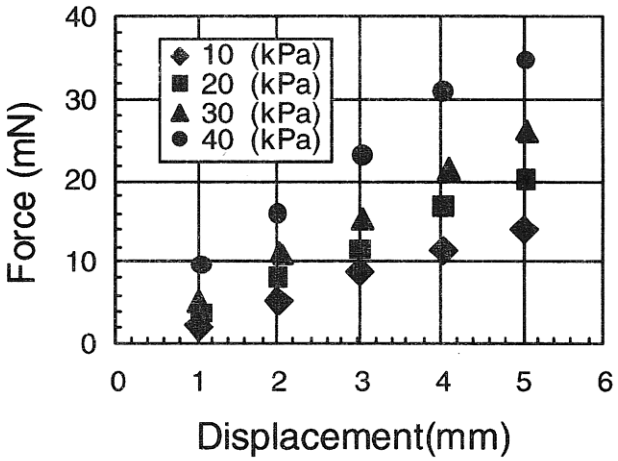

Fig.10 Measured relationship between force and displacement with varying the externally supplied pressure.

Table 1 A length dependence of the bending stiffness estimated through FEM analysis with applied pressure of 10 kPa and force of 5 mN.

Pressure (kPa)	Length 20 mm	Length 30 mm	Length 40 mm
	Width 20 mm	Width 20 mm	Width 20 mm
10	1.2 mm	2.5 mm	8.0 mm

confirmed that not to depend on the deformation speed of the device as shown in Fig. 7.

PNEUMATIC BALOON DEVICE

DESIGN

Figure 8 explains a mechanism of a single pneumatic balloon device using both schematic and cross-sectional views. The balloon swells by supplying a pressure, so that the required force to bend and stretch the device structure is expected to increase according to the supplied pressure. The fabricated pneumatic balloon device is composed of two 200 μm thick silicone rubber films sealed together at surrounding edges.

When a large number of pneumatic balloon devices with controllable stiffness are distributed on the surface of the deformable, it becomes possible to perform various deformations by controlling the surrounding boundary conditions.

The pressure will be supplied by a phase transformation of an enclosed medium in the balloon by Joule heating with a micro heater [6,7]. The feasibility of fluorinert phase transformation as a principle of the pressure supply was confirmed through bulging tests.

EXPERIMENTS

Figure 9 shows an experimental setup. A load cell and a laser displacement sensor were used to measure a force and a displacement, respectively.

Experimental results are shown in Fig. 10. The required force to bend the pneumatic balloon device increases according to the supplied pressure. The results indicate that it is possible to tune the bending stiffness of the pneumatic balloon device.

A length dependence of the bending stiffness was also estimated through FEM analysis. The length of the device was set at 20mm, 30mm, and 40mm with a constant width of 20mm. The analytical results are summarized in Table 1. Bending displacements at the same force and pressure were compared. The applied force was 5mN and the pressure in the cavity was 10kPa. The shorter length of the structure leads to a smaller

bending displacement. This result indicates that the characteristics of the device can be designed by the size of the device.

For comparison, a relation between the stretching force and the displacement with varying the externally supplied pressure were also measured. The required force to stretch the pneumatic balloon device slightly increases according to the supplied pressure.

CONCLUSION

Through analysis and experiments, it was confirmed that the tunable bending stiffness device can be realized by microfabrication technology using electrostatic force and pneumatic force. By miniaturizing the device and arranging them in stacked or array form, the performance of the device such as tunable range and distribution of the constraints can be improved.

ACKNOWLEDGEMENT

This research was supported in part by Mirai Kaitaku Project "JSPS-RFTF9600804".

REFERENCES

[1] C. P. Chou et. al., "Static and Dynamic Characteristics of McKibbn pneumatic artificial Muscles", ICRA'94, pp.281-286, 1994.

[2] H. M. Paynter, "Low-cost pneumatic Arthrobots powered by Tug-and-Twist polymer Actuators", Proc. Japan-USA Symposium on Flexible Automation, Vol.1, pp.107-110, 1996.

[3] T. Shimizu et. al., "Development of a Hexahedron Rubber Actuator", ICRA'95, pp.2619-2624, 1995.

[4] T. Niino et al., "Electrostatic Artificial Muscle: Compact, High-Power Linear Actuators with Multiple-Layer Structures", MEMS'94, pp. 130-135.

[5] K. Suzumori et al., "Microfabrication of Integrated FMAs using Stereo Lithography", MEMS'94, pp. 136-141.

[6] C. Grosjean et al., "Micro Balloon Actuators for aerodynamic control", MEMS'98, pp.166-171.

[7] J. Ok et al., "Pneumatically driven Microcage for Micro-objects in biological liquid", MEMS'99, pp. 459-463.